

Published in final edited form as:

Build Environ. 2021 July ; 199: . doi:10.1016/j.buildenv.2021.107888.

Evaluation of a four-zone indoor exposure model for predicting TCPP concentrations in a low-energy test house

Dustin Poppendieck^{1,*}, Mengyan Gong¹, Stephen Zimmerman¹, Lisa Ng¹

¹National Institute of Standards and Technology, USA

Abstract

Numerous chemicals have been detected in indoor environments that have potential impacts on occupant health and comfort. However, due to limited resources, it's infeasible to assess indoor exposure of each chemical for all indoor conditions through measurements alone. Hence, indoor exposure models have been developed to predict time-varied exposure for a wide range of sources and chemicals under different conditions. The *Indoor Environmental Concentrations in Buildings with Conditioned and Unconditioned Zones (IECCU)* model was developed by the United States Environmental Protection Agency. This study evaluated the predictive ability of the IECCU by comparing airborne tris(1-chloro-2-propyl) phosphate (TCPP) concentrations measured from 2013 to 2018 in a test house to modeled predictions. Inputs to IECCU included building and environment (i.e., air zone configuration and geometry, interzonal airflow rates and air temperature in each zone), parameters for both source (spray polyurethane foam (SPF)) and sinks (gypsum and wallboard), and simulation conditions. Simulations were conducted using three sets of inputs. Simulation 1 and 2 differed in using quantified versus design inputs for temperatures and airflow rates. Simulation 1 and 3 differed in the configured air zones in the IECCU model. Given the best available inputs (Simulation 1), IECCU predicted basement concentrations that were generally higher but within a factor of three of the measurements. The basement prediction/measurement ratios for all three simulations ranged from 0.5 to 8.3 and the average was 2.9, while the predicted concentrations in the living zone were generally lower but still within an order of magnitude of the measurements. The prediction accuracy decreased with time. For Simulation 1, predicted basement concentrations were on average 1.4 times higher than measurements in 2013 and 2014. However, the ratio increased to 4.7 in 2018. The design inputs of Simulation 2 resulted in greater discrepancy between measurements and predictions than the measured inputs of Simulation 1. In addition, Simulation 2 did not capture diurnal variation as well as Simulation 1. Comparisons of Simulation 1 and 2 demonstrate the importance of using accurate temperature and airflow model inputs for more accurately predicting concentrations. Furthermore, a sensitivity analysis indicated that to improve the accuracy of IECCU predictions for TCPP emission from SPF, efforts are needed to accurately measure the mass transfer parameters for SPF, especially the SPF/air partition coefficient and the initial TCPP concentration in SPF.

* corresponding author.

Disclaimer

Certain programs or materials are identified in this paper in order to specify the analysis adequately. Such identification is not intended to imply recommendation or endorsement by the National Institute of Standards and Technology, nor is it intended to imply that the program or materials identified are necessarily the best available for the purpose.

Keywords

Spray polyurethane foam (SPF); Indoor Environmental Concentrations in Buildings with Conditioned and Unconditioned Zones (IECCU) model; mass transfer coefficient; partition coefficient

Introduction

Over 100,000 different chemicals are manufactured every year (Levi and Cullen 2018), with many incorporated into products that are used in the indoor environment. The fate and transport of most of these chemicals in the indoor environment has not been measured or measured infrequently relative to relative to the large number of buildings and circumstances of building operation, occupant activity and weather conditions. Given that it is infeasible to measure emission of all chemicals from indoor sources in different environmental conditions, various models have been developed to predict the potential indoor concentrations of these chemicals.

The United States Environmental Protection Agency (USEPA) has developed and applied a range of models to predict the fate and transport of chemicals indoors, including IAQX, i-SVOC, and the *Indoor Environmental Concentrations in Buildings with Conditioned and Unconditioned Zones (IECCU)*. IAQX is a volatile organic compound (VOC) model that simulates multiple well-mixed zones and airborne chemical reactions. IAQX can be used to predict VOC emissions from solvents and coatings, along with diffusion-controlled VOC emissions from different materials (United States Environmental Protection Agency 2020b). Given the different chemical properties between VOCs and semi-volatile organic compounds (SVOC), a more general-purpose model, i.e., i-SVOC (Indoor SVOC), was developed to examine the fate and transport of SVOCs emitted from indoor sources by accounting for SVOC sorption to size aggregated particulate matter, settled dust and other sinks such as building materials and furnishings (United States Environmental Protection Agency 2020a).

The IECCU (United States Environmental Protection Agency 2020c) combines existing code in IAQX and i-SVOC and adds new components and methods, such as allowing time dependent airflow and temperature inputs from other models. IECCU requires 1) defining a building environment, including the air zones, outdoor and interzonal airflows and temperature in each zone, 2) describing sources and sinks, including location and surface area for both, source emission models, sink adsorption models and corresponding parameters, and 3) inputting simulation conditions, including initial air concentrations and simulation duration. IECCU allows nine types of air zone configurations for a building each consisting of up to three, well-mixed zones and an air handling unit “zone”. An example of a IECCU configuration is model that consists of a living zone, unheated attic and air handling unit. Each IECCU zone is described by a volume and surface areas of relevant materials. Time-varying temperatures in each zone, airflows between zones, and airflows between the zones and outdoors must be input to the model. These time-varying values may be generated using measurements or building airflow modeling programs. The model can vary the partition and diffusion coefficients of target chemicals for the sources can be with temperature fluctuations.

In this study, for the first time, the IECCU predictions were evaluated by comparing them with long-term measurements in a test house. The Net-Zero Energy Residential Test Facility (NZERTF) at the National Institute of Standards and Technology (NIST) was constructed as a testbed for evaluating the performance of low-energy designs, technologies, and construction methods (Pettit, Gates et al. 2014). The unoccupied 1316 m³ NZERTF has an open basement, two living space floors and an attic (insulated and air sealed at the roof, not the attic floor) connected to the 2nd floor via passive transfer grilles. The basement and first floor are also connected via passive transfer grilles. A heat recovery ventilator (HRV) provides 137 m³ h⁻¹ of mechanical ventilation to comply with ASHRAE Standard 62.2–2010 (ASHRAE 2010, Ng, Persily et al. 2015). Total outdoor air change rates, which included both the mechanical ventilation rate through the HRV and infiltration through the building envelope, range from 0.06 h⁻¹ to 0.19 h⁻¹ (Ng, Persily et al. 2015). The NZERTF building envelope uses a range of insulation products, including open cell spray polyurethane foam (SPF) (Poppendieck, Gong et al. 2017). SPF is a product that is produced on site by mixing methylene diphenyl diisocyanate with chemicals that include polyols, amines, blowing agents, surfactants, and flame retardants (Sebroski 2012, Poppendieck, Schlegel et al. 2016). The most common flame retardant in SPF is tris(1-chloro-2-propyl) phosphate (TCPP) and is typically present in the final product at levels between 2 % and 12 % by mass (Sebroski 2012, Estill, Slone et al. 2019, Gong and Poppendieck 2019).

TCPP has a boiling point between 200 °C and 248 °C (Xu, Yu et al. 2018, National Center for Biotechnology Information 2020) and may either be classified as a VOC or a SVOC (ASTM D8141). TCPP is found in a wide range of indoor products including flooring, furniture, toys, construction materials, curtains, foot-wear, leather products, paper and cardboard products, and electronic equipment (European Chemicals Agency 2020). TCPP has been reported to widely exist in different media in the indoor environment, including gas phase (Tokumura, Hatayama et al. 2017, Kim, Wang et al. 2019, Wang, Bao et al. 2020), dust (Wu, Yu et al. 2016, Peng, Tan et al. 2017, Tan, Peng et al. 2017, Tokumura, Hatayama et al. 2017, Ali, Ibrahim Ismail et al. 2018, Kim, Wang et al. 2019, Percy, La Guardia et al. 2020), particles (Schreder, Uding et al. 2016, Wang, Bao et al. 2020) and surfaces (Liu, Allen et al. 2016). Thus, humans are widely exposed to TCPP in indoor environments, which is supported by the fact that TCPP metabolites were detected in urine in multiple studies (Ding, Deng et al. 2019, Estill, Slone et al. 2019, Jayatilaka, Restrepo et al. 2019) and were present in urine at a detection frequency up to 60 % in the 2013–2014 National Health and Nutrition Examination Survey (NHANES) (Ospina, Jayatilaka et al. 2018). Health effects of TCPP exposure are currently being evaluated by the United States National Toxicology Program (National Toxicology Program 2020). However, TCPP has been reported to be related with adverse effects in cells and animals, including temporary DNA damage and viability decrease of peripheral blood mononuclear cells (Mokra, Bukowski et al. 2018, Bukowski, Wysokinski et al. 2019), proteins and metabolites alteration in rockfish (Ji, Lu et al. 2020) and dose-response immune stress in mussels (Wu, Zhong et al. 2018).

During construction of the NZERTF, SPF was applied in approximately January 2012 to the basement rim joists and to the rim joists between the 1st and 2nd floor. The basement SPF is not covered by any finish material. The 1st and 2nd floor rim joist SPF is isolated

from the 1st floor by wallboard and the 2nd floor by a plywood subfloor and wood flooring. Other than the rim joist SPF there are no other known sources of TCPP in the NZERTF (Poppendieck, Schlegel et al. 2016). Total TCPP airborne concentrations (particle and gas phase) were measured in the NZERTF basement, 1st floor, and 2nd floor over a period of five years (2013 to 2018) (Poppendieck, Gong et al. 2019). In addition, since 2013, data with resolution of seconds has been collected at the NZERTF on electricity use, water use, HVAC system performance, and thermal comfort (Healy, Fannery et al. 2017, Healy, Chen et al. 2018), including temperature and flow data that may be used as direct or indirect inputs to the IECCU model. Hence, the TCPP measurements in NTZERTF with a single source of SPF serve as a unique test case for evaluation of the IECCU and other exposure models.

The objective of this effort is to evaluate long-term airborne TCPP concentration predictions from the IECCU model by comparing the predictions with measurements.

Methods

Calculating airborne TCPP concentrations using the IECCU model requires the determination of input parameters for the building and indoor environment (i.e. air zones, temperature and interzonal airflows), sources and sinks of TCPP, and simulation conditions (initial condition and simulation duration). Three simulation cases were performed with combinations of two air zone configurations and two different sets of temperature and airflow inputs (Table 1). Simulations 1 and 2 were compared to examine the difference between the quantified versus design values of airflow and temperature data. Simulations 1 and 3 were compared to examine the difference between the building configurations (Attic versus Floorspace). This section describes the details of these building configurations and differences between quantified and design input data for building operations.

IECCU Air Zone Configurations

The IECCU can be used to model up to three conditioned zones and an HVAC zone. The HVAC zone is the ductwork. In this study, two air zone configurations for the NTZERTF were modeled (Figure 1). The Attic configuration was a four-zone configuration that did not include the volume between the 1st and 2nd floors. The living zone in the Attic configuration includes the combined volumes of the 1st and 2nd floors. The Floorspace configuration was a four-zone configuration that included the 1st and 2nd floorspace volume as a zone and combined the attic, 1st and 2nd floors into the living zone. The floorspace zone is the air gap between the ceiling of the first floor and floor of the second floor. Both configurations have identical basement and HVAC zones. For both configurations, the directional airflows indicated by arrows in Figure 1 are the airflows input into the IECCU model. Air entering zone j from zone i (Q_{ij}) does not need to be equal to the opposite airflow Q_{ji} . The airflow (Q) subscripts in Figure 1 are as follows: Outside (O), Attic (A), Living Area (L), Basement (B), HVAC system (H), Floorspace (F).

In the Attic configuration, a TCPP source of 15 m² SPF was located in the basement only, represented by the hashed blocks in Figure 1. The SPF in the rim joists between the 1st and 2nd floor was not included in the Attic configuration due to that volume having a limited airflow to other zones and the IECCU model limiting the model to three non-HVAC zones. In

the Floorspace configuration, TCPP sources of 15 m² SPF were located in both the basement and floorspace.

Design and Quantified IECCU Temperatures and Interzonal Airflows

The IECCU model requires input of hourly airflow rates across the building envelope to and from each zone (Q_{O_i}), the airflow rates between zones (Q_{ij} and Q_{ji}), exhaust airflow rates, outdoor ventilation rates, HVAC system airflow rates, and temperatures in each zone. Two sets of input data for the hourly airflows and temperatures were created: “design” and “quantified”.

The “design” IECCU input data for the building size, airflow rates, temperatures and source sizes are estimated or assumed based on design information. This scenario could represent design intent. The “quantified” input IECCU data consist of airflow rates and temperatures that were either directly measured or modeled as described below. This scenario represents the best available data for predicting indoor exposure.

Design Temperatures.—It was assumed that the indoor temperatures and HVAC temperatures were equal to the heating setpoint (21.1 °C) between November and April, and equal to the cooling setpoint (23.9 °C) between May and October (Fanne, Payne et al. 2015).

Quantified Temperatures.—Temperatures in the HVAC system (return and supply) were recorded every 3 s when the fan was running and every 10 s otherwise using Type-T thermocouples with a range of – 10 °C to 55 °C and a manufacture specified uncertainty at the 95 % confidence level of ± 0.6 °C (Davis et al. 2014). There are three thermocouples in the HVAC return. The recorded values of these sensors were integrated and averaged at hourly timesteps to create the temperature data inputs for the temperature of Q_{LH} . There are three thermocouples in the HVAC supply. The recorded values of these sensors were integrated and averaged at hourly timesteps to create the temperature data inputs for temperature of the Q_{HL} and Q_{HB} .

Temperatures inside the NZERTF were recorded every 1 min using Type-T thermocouples with a range of 13 °C to 30 °C and a manufacture specified uncertainty at the 95 % confidence level of ± 0.2 °C (Davis et al. 2014). The temperature input for the living zone in the IECCU model were determined by integrating and averaging measurements from 16 thermocouples inside 1st and 2nd floors of the test house. The temperature input for the basement zone in the IECCU model consisted of integrated and averaged measurements from four thermocouples in the basement of the test house. Lastly, the temperature input for the Attic zone in the IECCU model consisted of integrated and averaged measurements from four thermocouples inside the attic of the test house. The values recorded every minute from all the sensors in the zone were integrated and averaged at hourly timesteps to create the temperature data inputs for each zone. Intentional and unintentional events caused the data acquisitions systems to record erroneous data for less than 6 % of the time over the five years of data acquisition (see Supporting Information). These erroneous data points were replaced using either the previous (or the following) day’s data from the same timeframe if more than five data points were missing or by averaging the data points before and

after the erroneous data point if fewer than five data points were missing. The variations of measured basement zone temperatures for the three simulations are illustrated in Figure S.3. Temperatures for Simulation 2 only varied seasonally, but the basement temperature for Simulation 1 and 3 changed every hour and had a relative standard deviation of 5 %.

Design Airflows.—The design airflow rates were based on design specifications for the NZERTF without considering any measured data. For the HVAC airflow rates, it was assumed that the system operated two-thirds of the hour when the outside temperature was equal to the heating design temperature (HDT) or cooling design temperature (CDT) of the location. In Baltimore, MD, the HDT = -7.6 °C and CDT = 33.0 °C (ASHRAE 2017). Figure S.2 shows that between the heating setpoint of 21.1 °C and the HDT, and between the cooling setpoint of 23.9 °C and the CDT, the operation of the HVAC system was varied linearly from 0.0 to 0.67 of the maximum airflow in the manufacturer’s specifications. For cooling, the maximum airflow is 1710 m³h⁻¹, and for heating, the maximum airflow is 1026 m³h⁻¹.

For the design data set, it was assumed that the air leaving and coming into the test house across the building envelope (Q_{oi} and Q_{io}) was equal to the infiltration credit in ASHRAE Standard 62.2–2016. For a single detached home, the infiltration credit ($Q_{inf,62.2}, L s^{-1}$) is:

$$Q_{inf,62.2} = \frac{NL \times wsf \times A_{floor}}{1.44} \quad (1)$$

where NL is the normalized leakage (–), wsf is the weather shielding factor (–), and A_{floor} is the floor area (m²). For the NZERTF, $Q_{inf,62.2}$ is 7 L/s. It was also assumed that the HRV supply and exhaust airflow rates were equal to the rate required by Standard 62.2, 137 m³ h⁻¹. Because interzonal airflow is not a design feature, these airflow rates were estimated from data in Ng, Kinser et al. (2019), where the authors performed pressurization fan tests to determine the leakage of interior floors, doorways, and passive transfer grilles. The results were then input into a CONTAM model of the house, as described below. Using local weather data, airflow was simulated for a year. The annual average interzonal values reported in Ng, Kinser et al. (2019) were input into the IECCU as a constant value. The variations of design airflows for Simulation 2 are illustrated in Figure S.5.

Quantified Airflows.—The quantified inputs were created from a combination of measurements and simulation results using measurements as input. Pressurization tests were conducted to determine the exterior leakage area of the building envelope and interzonal leakage area through the interior floors (Ng, Kinser et al. 2019). The leakage areas along with the measured indoor and outdoor temperatures, wind speed and direction, HVAC system airflow rates, and HRV airflow rates were used as inputs to a CONTAM model of the house. CONTAM is a multizone airflow simulation software developed at NIST that incorporates airflow physics to determine building airflows and indoor contaminant concentrations (Dols and Polidoro 2015). CONTAM has been validated in terms of program integrity (Haghighat and Megri 1996), and comparisons with laboratory experiments (Haghighat and Megri 1996) and field studies (Chung 1996, Haghighat and Megri 1996,

Emmerich 2001, Emmerich, Nabinger et al. 2004). A previously developed model of the NZERTF house was used (Poppendieck, Khurshid et al. 2016) (Figure S.1). Thus, the airflows through the building envelope (Q_{AO} , Q_{OA} , Q_{LO} , Q_{OL} , Q_{BO} , Q_{OB}) and between zones (e.g., Q_{AL} , Q_{LA} , Q_{BL} , Q_{LB}) were simulated using CONTAM and provided as inputs to IECCU. The model also took into account times when the basement door was open.

During testing, the HRV operated on constant and intermittent schedules, and the airflow rates varied between $137 \text{ m}^3 \text{ h}^{-1}$ and $205 \text{ m}^3 \text{ h}^{-1}$. The higher HRV airflow rates were measured when the NZERTF was operated at higher than the Standard 62.2 specification to investigate energy and air quality impacts. The HRV operation schedule was used to derive airflow rates to input into CONTAM. All HRV supply air was delivered to the living zone.

Quantified HVAC airflow rates were derived from measurements taken by a differential air pressure transducer, which monitors the indoor unit air pressure drop and external static pressure (Davis, Healy et al. 2014). The air pressure differential measurement had a range of 0 Pa to 187 Pa and a manufacturer specified uncertainty at the 95 % confidence level of $\pm 0.8 \%$ of reading. The measured differential was then used to calculate the airflow rates as described in Davis, Healy et al. (2014) for the HVAC system and recorded every 3 s when the indoor fan was running and every 10 s when the indoor fan was not running. The fraction of the HVAC airflow going to the basement (Q_{HB}) compare to the living zone (Q_{HL}), 10%, was determined using a balometer periodically throughout the study period (manufacturer stated accuracy of $\pm 3\% + 8.5 \text{ m}^3 \text{ h}^{-1}$). The recorded values of this sensor were integrated at hourly timesteps to create the inputs for the Q_{Hi} and Q_{H} airflows in IECCU. Erroneous airflow data were recorded less than 5 % of the time over the five years of data acquisition (see Supporting Information). These erroneous data points were replaced in the same manner as the temperature data. The variations of quantified airflows for Simulation 1 and Simulation 3 are illustrated in Figure S.4 and Figure S.6, respectively.

IECCU Sources

TCPP emission from SPF was simulated using the diffusion model in IECCU, which requires user input for the initial TCPP concentration in the SPF source (C_0), the TCPP partition coefficient between SPF and air ($K_{\text{SPF/air}}$), the TCPP diffusion coefficient in SPF (D_{SPF}) and the convective mass transfer coefficient on the SPF surface ($h_{m, \text{SPF}}$) (Table 2).

Initial TCPP concentration in SPF.—The initial TCPP concentration in the SPF (C_0) was estimated from mass fraction measurements for similar open cell SPF (Poppendieck, Gong et al. 2017). The density of the open cell SPF in the NZERTF was 7 kg m^{-3} (Poppendieck, Gong et al. 2017). The initial TCPP concentration of similar open cell SPF with a density of 8.3 kg m^{-3} was 12.5 % TCPP by mass (Gong and Poppendieck 2019). This value is similar to ranges reported in formulations by Sebroski (2012) (8 % to 15 %). The bulk TCPP concentration in SPF remains relatively constant over the simulation time frame given the relatively small TCPP mass that it emits (1 g y^{-1} to 3 g y^{-1} , based upon $10 \mu\text{g m}^2 \text{ h}^{-1}$ Poppendieck, Schlegel et al. (2016)) compared to approximately the 6 kg TCPP mass total in the SPF in the building.

Partition coefficient.—There are various methods proposed to estimate $K_{\text{SPF/air}}$ based on other parameters such as the octanol-water partition coefficient (Huang and Jolliet 2019). Estimated $K_{\text{SPF/air}}$ values were used for simulating TCPP emission from SPF based on existing literature (Bevington, Guo et al. 2017, Tian, Sebroski et al. 2017). However, these estimated values vary by up to three orders of magnitude depending on the estimation method used (Tian, Sebroski et al. 2017). In addition, the available empirical correlations for estimating $K_{\text{SPF/air}}$ were derived without measurement data for the TCPP partition coefficient between either SPF or non-SPF polyurethane foam and air.

To the best of our knowledge, no measured value for the TCPP partition coefficient between open cell SPF and air ($K_{\text{SPF/air}}$) has been reported in the literature. Liang, Liu et al. (2018) measured the TCPP $K_{\text{SPF/air}}$ for a closed cell SPF sample (5.3×10^7 at 23 °C). However, the $K_{\text{SPF/air}}$ for open cell is likely to be significantly smaller than the $K_{\text{SPF/air}}$ for closed cell SPF given that the airborne TCPP concentrations in microchambers with open cell SPF were reported to be two orders of magnitude higher than the concentrations in microchamber with closed cell SPF (Poppendieck, Gong et al. (2017)).

The only measurement for TCPP partition coefficients between open cell polyurethane foam and air was reported by Liu, Allen et al. (2016). In Liu et al. (2016), airborne TCPP concentrations adjacent to non-SPF open cell polyurethane foam surface were first measured and then the partition coefficients were derived by combining the measured concentrations with TCPP vapor pressure reported in the literature. Liu, Allen et al. (2016) summarized the reported TCPP vapor pressures, most of which ranged from 0.0014 Pa to 1.2 Pa at 25 °C and suggested the variation is due to impurities. As a result, Liu, Allen et al. (2016) choose 0.014 Pa from the European Union Risk Assessment Report (2008) to calculate the partition coefficients. Given that the partition coefficient between non-SPF type of open cell polyurethane foam and air by Liu, Allen et al. (2016) was the closest measured approximation to $K_{\text{SPF/air}}$, that value was used as $K_{\text{SPF/air}}$ in this study (Table 2). This value, 4.4×10^6 at 25 °C, is within the range of values estimated by Tian et al. (2017)), but lower than the 5.3×10^7 at 23 °C measured by Liang, Liu et al. (2018) for closed cell SPF. In addition, the variation of partition coefficient as a function of temperature determined by Tian et al. (2017) and included in IECCU was used to calculate $K_{\text{SPF/air}}$ at other temperatures.

Diffusion coefficient in SPF.—The diffusion coefficient (D_{SPF}) at 25 °C used in this study (Table 2), i.e. $8.6 \times 10^{-11} \text{ m}^2 \text{ h}^{-1}$, is an average value for non-SPF open cell polyurethane foams measured by Liu, Allen et al. (2016), as there are no available values for TCPP diffusion coefficients in SPF in the literature. The TCPP diffusion coefficients by Liu, Allen et al. (2016) were determined in part using the correlation between diffusion coefficient ratio and molecular weight ratio of two chemicals and using tris(2-chloroethyl) phosphate (TCEP) as the reference chemical. In addition, D_{SPF} at other temperatures were calculated using the equation relating diffusion coefficient and temperature determined by Tian et al. (2017) that is included in IECCU.

Convective mass transfer coefficient on the SPF surface.—The convective mass transfer value (h_m , m h^{-1}) was calculated based upon the Sparks method as explained by Guo (2005):

$$h_m = 0.33D_a L^{-1/3} \left(\frac{u\rho}{\mu} \right)^{2/3} \left(\frac{3600s}{h} \right) \quad (2)$$

where D_a is the TCPP diffusion coefficient in air ($\text{m}^2 \text{s}^{-1}$), L is the characteristic length (m), v is the mean air velocity (m s^{-1}), ρ is the density of air (kg m^{-3}), and μ is the viscosity of air ($\text{kg m}^{-1} \text{s}^{-1}$). The D_a , ρ and μ values were calculated at the average temperature value for the simulations using USEPA's PARAMS (Guo 2005). For the diffusion coefficient, D_a , the FSG1 method in PARAMS software was chosen. The relative humidity was assumed to be 50 % for the air density calculation, ρ . The mean air velocity value of 0.05 m s^{-1} was chosen from the range presented in Guo (2005). The characteristic length, L , was calculated as the square root of the SPF surface area (Table 2).

IECCU Sinks

Sorption of TCPP to surfaces was only simulated for surfaces where TCPP partition and diffusion coefficients were available in the literature (Liu, Allen et al. 2016), i.e., gypsum wallboard and concrete. The surface areas of the sorbing surfaces in each zone were measured and are listed in Table 2. The thickness of gypsum board and concrete was assumed to be 0.012 m and 0.1 m, respectively. The partition and diffusion coefficients used were from Liu, Allen et al. (2016) (Table 2). The convective mass transfer coefficient was calculated in the same manner as described in the source section. For walls the characteristic length, L , was determined as the square root of the area of the walls in the zone divided by four. The mass transfer coefficients h_m (gypsum -walls) and h_m (gypsum -ceiling) were both 0.53 m h^{-1} . The limitations discussed in the source section for these parameters also applies to the sink coefficients. In addition, the partition and diffusion coefficients for sinks do not vary with temperature in the IECCU.

The major surfaces that were not included in this analysis were the finished wood floors on the 1st and 2nd floors and the exposed unfinished wood on the ceiling of the basement and in the attic.

IECCU Simulation conditions

Simulation Periods.—IECCU can run simulations at a resolution of 1 h but can only output a maximum of 5000 data points. For consistency all three simulations began on July 1st, 2013, run for 45000 h and generated output data every 9 h. For comparison, airborne TCPP concentration measurements typically lasted between 3 h and 4 h.

The SPF was applied to the building around January 1st, 2012 but the collection of NZERTF airflow and temperature data started on July 1st, 2013. A preliminary analysis showed that starting simulations on July 1st, 2013 (when the building operation data were first being recorded in the NZERTF) rather than January 1st, 2012 (when the SPF was applied) had

less than a $1 \mu\text{g m}^{-3}$ impact on the airborne concentration results over the time period of measured airborne TCPP samples (Figure S.7).

Initial TCPP concentration in air.—The IECCU model allows a non-zero initial concentration of a chemical to be used as a model input. Because this value was not measured, the initial concentration in air on July 1st, 2013 in the basement was estimated to be $4.3 \mu\text{g}/\text{m}^3$ by multiplying the TCPP concentration measured in the basement on July 1st, 2014 by the ratio of average measured TCPP concentrations in the air in 2014 and 2015 (ratio=1.5). The initial airborne TCPP concentration in the air on July 1st, 2013 in the living, floorspace, and HVAC zones of the IECCU were assumed to be half of the TCPP concentration in the basement. The initial concentration in the Attic zone of the IECCU was assumed to be a quarter of the TCPP concentration in basement.

Measured TCPP Concentrations

Total airborne (gas and particle phase) TCPP measurements were made in the basement and 1st floor of the NZERTF between 2014 and 2018 (Poppendieck, Gong et al. 2019). Triplicate or duplicate samples were taken using dual Tenax tubes sampled at a rate of 50 mL min^{-1} for 3 h to 4 h. The dual sorbent tubes were connected in series with the second tube used to check for breakthrough of the first tube. Sample tubes were analyzed using thermal desorption, gas chromatograph mass spectrometer analysis. The two primary TCPP conjugates were quantified using methanol diluted neat standards spiked onto sorbent tubes. Method detection limits for TCPP in air were $0.21 \mu\text{g m}^{-3}$ to $0.70 \mu\text{g m}^{-3}$. Details of the analysis method are summarized in Poppendieck, Gong et al. (2019). For days with triplicate samples (21 out of 29 days), standard deviations were determined and are displayed in the result figures. For days with duplicate samples, only the average value is displayed.

From July 18, 2014 through July 28, 2014, two perturbations to the NZERTF operation were performed as described in Poppendieck, Ng et al. (2015). First, the temperature was raised by $8 \text{ }^\circ\text{C}$ ($32 \text{ }^\circ\text{C}$) for five days with normal ventilation rates (0.22 h^{-1} , July 18, 2014 through July 22, 2014). Next, the building was allowed to cool for four days (July 23, 2014 through July 26, 2014). Finally, the temperature was restored to $24 \text{ }^\circ\text{C}$, and the ventilation rate was decreased to 0.02 h^{-1} for two days (July 27, 2014 through July 28, 2014). These changes are reflected in Simulations 1 and 3. TCCP concentrations were measured after at least two days of the perturbations, allowing the NZERTF to reach steady state operation.

Model fit assessment

The IECCU model fit was assessed by comparing modelled TCPP concentrations to measured values in the same zone and time period using normalized mean square error (NMSE) and linear correlation analysis as described in ASTM Guide D5157 (ASTM 2019). The guide defines models to be “indicative of adequate model performance” when the linear correlation coefficient is greater than 0.9, the regression slope is between 0.75 and 1.25, the intercept is less than 25 % of the average concentration, and the NMSE is not larger than 0.25.

Sensitivity analysis

A sensitivity analysis was conducted by varying one parameter at a time while keeping other parameters at baseline values. The parameter values for Simulation 1 were used as baseline values. A total of 20 different parameters were varied individually to indicate the impact of each parameter on the IECCU model outputs. Four airflow related parameters along with sixteen mass transfer related parameters were varied.

Interzonal leakage areas in single-family residential buildings have been shown to be up to ten times greater than the exterior leakage areas (Emmerich, Gorfain et al. 2003, Ng, Kinser et al. 2019). Ng, Kinser et al. (2019) calculated relative measurement 95 % confidence intervals of less than 10 % for interzonal leakage areas in the NZERTF. To be conservative interzonal leakage areas (between the basement and living zones and the living and attic zone) were varied by a factor of two larger and smaller than the values used in Simulation 1. Exterior leakage areas and the fraction of HVAC going to the basement were simulated at values 20 % larger and smaller than the baseline values.

As noted above, estimated SPF partition coefficients vary by three orders of magnitude (Tian, Sebroski et al. 2017). Furthermore, the vapor pressure used for estimating the partition coefficients used as the baseline value for Simulation 1 may vary by seven orders of magnitude (Liu, Allen et al. 2016). In addition to the variability in vapor pressure used in the calculation by Liu, Allen et al. (2016), there was also sample variability. Partition coefficients for duplicate non-SPF polyurethane foam samples and gypsum wallboard had differences of 30 % and 26 %, respectively. Diffusion coefficients for duplicate non-SPF polyurethane foam samples had a difference of 83 %, while the difference was 75 % for gypsum wallboard. Given these variabilities, the sensitivity of partition and diffusion coefficients for SPF, gypsum wallboard and concrete were analyzed at values one order of magnitude larger and smaller than the baseline values used in Simulation 1.

When estimating the initial TCPP concentration used in this study, TCPP in SPF by mass was assumed to be 12.5 % (Gong and Poppendieck 2019). Open cell SPF formulations by Sebroski (2012) ranged from 8 % to 15 %. As a result, the initial TCPP concentration was varied by a factor of two in this sensitivity analysis. Of the parameters that impact the mass transfer coefficients (Equation 2), the mean air velocity is the only parameter that has more than 5 % variability at the temperature ranges in the NZERTF basement. Mean air velocity above a surface can range from 0.05 m s⁻¹ to 0.1 m s⁻¹ (Guo 2005). This range correlates to a range of mass transfer coefficients for SPF from 0.81 m h⁻¹ to 1.28 m h⁻¹ (Simulation 1, run at 21 °C, had a baseline mass transfer coefficient value of 0.81 m h⁻¹). As a result, the mass transfer coefficients were varied by a factor of two larger and smaller than the values used in Simulation 1.

The surface areas and thicknesses of SPF, gypsum wallboard and concrete were tested at values 20 % larger and smaller than the baseline values. This variation may result from measurement error, roughness of SPF surface, or estimation error for the gypsum area in the attic.

Results and Discussion

Comparison of IECCU simulation predictions and measurements.

The measured airborne TCPP concentrations in the basement were first compared with predictions from Simulation 1 (best available inputs) (Figure 2). Simulation 1 captured the concentration increase and decrease during the perturbation period in July 2014 (Figure S.9). However, Simulation 1 generally predicted higher concentrations than the measurements in the basement. In general, basement TCPP concentrations predicted using quantified inputs (Simulation 1) are $2 \mu\text{g m}^{-3}$ to $4 \mu\text{g m}^{-3}$ lower than predicted values using design inputs (Simulation 2). The abrupt increases and decreases in the Simulation 2 data correspond to the seasonal temperature changes associated with the thermostat setpoints in all zones: $23.9 \text{ }^{\circ}\text{C}$ in May to October and $21.1 \text{ }^{\circ}\text{C}$ the rest of the year (average $22.5 \text{ }^{\circ}\text{C}$). The average temperature of the basement zone in Simulation 1 was $21.1 \text{ }^{\circ}\text{C}$ (standard deviation = $1.1 \text{ }^{\circ}\text{C}$). This $1.4 \text{ }^{\circ}\text{C}$ average temperature difference may contribute to the basement concentration differences between Simulation 1 and Simulation 2 as temperature increase will decrease the partition coefficients and increase the diffusion coefficients, which result in 10 % higher emission rates on average (Figure S.8).

The predictions by Simulation 2 do not capture the daily concentration variations and general trend of measurement as well as Simulation 1 does. The typical daily variation of basement TCPP concentration due to diurnal temperature and airflow variations in Simulation 1 was $0 \mu\text{g m}^{-3}$ to $2 \mu\text{g m}^{-3}$ (inset Figure 2). For example, on June 6th, 2014 (06/06/14 on Figure 2), the maximum temperature difference was $0.5 \text{ }^{\circ}\text{C}$ and the maximum airflow difference for Q_{LB} , Q_{BL} , Q_{LH} , Q_{HL} and Q_{HB} were $0 \text{ m}^3 \text{ h}^{-1}$, $81 \text{ m}^3 \text{ h}^{-1}$, $829 \text{ m}^3 \text{ h}^{-1}$, $748 \text{ m}^3 \text{ h}^{-1}$, and $81 \text{ m}^3 \text{ h}^{-1}$, corresponding to a $2 \mu\text{g m}^{-3}$ diurnal concentration variation in Simulation 1. However, on the same day (June 6th, 2014), the TCPP concentration variation predicted by Simulation 2 varied by less than $0.1 \mu\text{g m}^{-3}$, while the diurnal temperature difference was zero and the maximum airflow differences for Q_{LB} , Q_{BL} , Q_{LH} , Q_{HL} and Q_{HB} were $0 \text{ m}^3 \text{ h}^{-1}$, $0 \text{ m}^3 \text{ h}^{-1}$, $330 \text{ m}^3 \text{ h}^{-1}$, $281 \text{ m}^3 \text{ h}^{-1}$, and $50 \text{ m}^3 \text{ h}^{-1}$. The difference between design and quantified input data becomes more obvious when the actual temperature and airflow conditions varied significantly in a short period of time, such as the perturbation period in July 2014. Overall, the differences between Simulation 2 predictions and measurements ratios of 1.0 to 8.3 were larger than the differences between Simulation 1 predictions and measurements ratios of 0.5 to 5.4. This indicates the importance of accurate temperature and airflow inputs for estimating TCPP concentrations and exposure, especially for short-term exposure.

For point-to-point comparisons, the concentrations closest in time to the sampling starting point were selected from the Simulation 1 output. The ratios between predictions and measurements in the basement increased with time. In 2014 the average concentration ratio was 1.6 (standard deviation = 0.7, $n = 12$); in 2015, the average ratio was 2.9 (standard deviation = 0.7, $n = 4$); in 2016, the ratio was 3.6 ($n=1$); in 2018, the average ratio was 4.7 (standard deviation = 0.5, $n = 5$). The change of in the ratio is consistent with the fact that the measured concentrations in the basement decreased 50 % between 2014 (average of non-perturbation samples = $2.77 \mu\text{g m}^{-3}$, standard deviation = $0.18 \mu\text{g m}^{-3}$, $n = 7$) and 2018

(average = $1.29 \mu\text{g m}^{-3}$, standard deviation = $0.21 \mu\text{g m}^{-3}$, $n = 12$), while the predictions only decreased 12 %.

The short-term temperature perturbation from July 18, 2014 through July 22, 2014 resulted in increased predicted TCPP concentrations for both Simulation 1 and 3 (Figure S.9). The ratio between the measurements (taken on July 22, July 23, July 25 and July 26, 2014) and the predicted concentrations averaged 1.3 for both simulations. When the house ventilation rate was reduced and the temperatures returned to normal operation conditions (July 29, 2014), the measured and predicted concentrations reduced and had an average ratio of 1.2. Measurements taken on July 25, 2014 and July 26, 2014, when the building was transitioning to cooler internal temperature settings, were higher than the predictions (average measured to predicted ratio was 0.5 for Simulation 1 and 3). This is likely due to the models accounting for high HVAC airflows to the basement due to cooling conditions. Overall, comparisons between predictions and measurements during and shortly after the perturbation period demonstrates that IECCU can respond to changes of input temperature and airflow data on a time scale of days.

Simulation 1 and 3 differed in the building configurations (Attic and Floorspace, Figure 1) and the location and amount of SPF. The temperature and airflow inputs were prepared separately for Simulation 1 and 3 as described in Methods, while all other parameters were consistent between the simulations. Figure 2 shows that the basement TCPP concentration predictions by Simulation 3 were, on average, 12 % lower than predictions from Simulation 1.

Figure 3 shows that the measured TCPP concentrations in the living zone from Simulation 3 were, on average, 32 % higher than the predictions from Simulation 1. The average airflows between the floorspace and living zone (Q_{LF} and Q_{FL}) were small, i.e. $0.3 \text{ m}^3 \text{ h}^{-1}$ and $0.4 \text{ m}^3 \text{ h}^{-1}$, compared to the average Q_{BL} ($57.2 \text{ m}^3 \text{ h}^{-1}$). This may explain why the emission from the 15 m^2 SPF source in the floorspace did not significantly increase the TCPP concentrations in other zones, even though the emission rates from SPF in the floorspace were on average 18 % higher than the emission rates from SPF in the basement (Figure S.8). The differences between individual airflows for Simulation 1 and 3 were less than $0.5 \text{ m}^3 \text{ h}^{-1}$ except the airflow from the basement to living zone (Q_{BL}). The average Q_{BL} ($82.3 \text{ m}^3 \text{ h}^{-1}$) for Simulation 3 was higher than the average Q_{BL} ($57.2 \text{ m}^3 \text{ h}^{-1}$) for Simulation 1. This is consistent with the lower predicted concentrations in the basement and the higher predictions in the living zone by Simulation 3 compared to Simulation 1.

All simulations predicted concentrations lower than the measurements in the living zone (Figure 3). In 2014 the average living zone concentration ratio between Simulation 1 prediction and measurement was 0.5 (standard deviation = 0.1, $n = 3$); in 2015, the average was 0.4 (standard deviation = 0.1, $n = 4$). The fact that simulation predictions were lower than the measurements in the living zone, but higher than the measurements in the basement indicates that the input for airflows, especially airflow between the basement and the living zone may not be accurately quantified. These inaccuracies may be due to difficulties in the measurement of interzonal airflows and the corresponding measurement errors (Ng et al., 2018). The difference between the predictions and measurements may also be partly due to

the uncertainty of other inputs including temperature, building configuration, and parameters related to sources and sinks. In addition, only gypsum and concrete were included as the adsorption surfaces in the simulations in this study, while the predicted concentrations in the basement may decrease if adsorption to other surfaces, such as wood and furniture, were included in the simulations.

Model fit assessment

Each simulation was evaluated by comparing simulated and measured TCPP concentrations using metrics described in ASTM Guide D5157 (ASTM 2019), i.e., normalized mean square error (NMSE), correlation coefficient, slope and intercept (Table 3). Simulation 1 and 3 had similar performance, with both much better than Simulation 2. However, based on the four performance metrics, all three simulations don't meet the suggested adequate performance criteria as described in ASTM Guide D5157 (ASTM 2019) when compared to measured airborne TCPP concentrations in the basement. The poor predictive performance may be due to both the error related to the measured data and error related to IECCU simulations. Besides the HVAC zone, only three zones are allowed in IECCU, so some zones in the NZERTF had to be combined. This may result in discrepancy between the real airflows and temperatures in the NZERTF and the input airflows and temperatures used in the IECCU model. In addition, as described in the methods section, most of the parameters, especially the ones related to sources and sinks, may have large uncertainties, which will influence the IECCU predictions. The influences of input parameter uncertainty on IECCU prediction are discussed in more detail in the sensitivity analysis section.

Parameter sensitivity analysis.

A sensitivity analysis was conducted for 20 parameters by varying one parameter at a time as described in the Methods. For each parameter, two simulations were run by setting a high and low value for that parameter while keeping all other inputs the same as Simulation 1 (baseline). Variations of the predicted concentrations in the basement when the input parameters are varied are summarized in Table S.2. Figure 4 shows that as C_0 increases, the predicted TCPP concentration increases proportionally and the relative change of TCPP concentration doesn't vary with time. The Biot number divided by the partition coefficient compares the resistance of the convective mass transfer over a material surface to the mass transfer resistance of diffusion within that material (ASTM 2017). If the ratio is greater than 35, then emission from the material will be controlled mainly by diffusion within the material, while if the ratio is less than 1, then the emission will be controlled primarily by diffusion of the chemical from the surface to the bulk air. The $Biot/K_{SPF/a}$ ($(h_{m, SPF} L_{SPF}/D_{SPF})/K_{SPF/a}$) for SPF in the baseline Simulation 1 was 22, which indicates both the diffusion process and convective mass transfer process can be rate controlling steps for TCPP emission from SPF. Hence, as shown in Table S.2 and Figure 5 through Figure 7, the emissions of TCPP from SPF are sensitive to all the mass transfer parameters, i.e. the partition, diffusion, and mass transfer coefficient ($K_{SPF/a}$, D_{SPF} , and $h_{m, SPF}$). As $K_{SPF/a}$ increases, the predicted TCPP concentration decreases (Figure 5), while as $h_{m, SPF}$ and D_{SPF} increase, the predicted TCPP concentration increases (Figure 6 and Figure 7). The relative change of TCPP concentration due to the change of $K_{SPF/a}$ (Figure 5) decreases with time. This is due to the fact that when $K_{SPF/a}$ decreased by a factor of ten, the $Biot/K_{SPF/a}$

increased to 220 (Table S.3). Hence, the emissions were mainly limited by diffusion in the SPF and, therefore, the predicted concentrations decayed significantly during the initial periods (blue line in Figure 5). Similarly, when D_{SPF} decreased and $h_{\text{m, SPF}}$ increased, the $\text{Biot}/K_{\text{SPF/a}}$ also increased (220 and 43 respectively) so that the relative resistance of the internal diffusion process increased, and thus the decay of the concentration in the early period increased (blue line in Figure 6 and orange line in Figure 7).

As the area of SPF (A_{SPF}) increases, the predicted TCPP concentration increases proportionally (Figure S.16). In contrast, as A_{concrete} and A_{gypsum} increase (Figure S.17 and Figure S.18), the TCPP concentration predictions decrease since the sink sorption increases as their areas increase. Similarly, as the sinks' diffusion coefficient increases, or partition coefficient increases, or convective mass transfer coefficient increases, the sorption to sinks increases which results in lower predictions (Table S.2).

Increasing the fraction of HVAC airflow going to the basement decreased the predicted basement concentrations (Figure S.19), although the relative impact on the basement concentrations was less than the impact of SPF mass transfer parameters (Table S.2). Changing the leakage areas input into the CONTAM model changed the average predicted concentrations by less than 1 % (Table S.2).

The sensitivity analysis also allows comparison of the relative importance of the 20 analyzed parameters. Figure 8 ranks the change in the average concentration for the high and low values compared to the baseline Simulation 1 average concentration. The elasticity score (relative change of output compared to the relative change of input parameter) shown in Figure S.21 shows a similar trend in the parameters. For both analyses the model is most sensitive to the SPF/air partition coefficient ($K_{\text{SPF/a}}$) and the initial concentration of TCPP in the SPF (C_0). The predictions are not sensitive to the variation of the thickness of SPF, gypsum and concrete (Table S.2, Figure S.20). This indicates that emission of TCPP from SPF is not limited by the diffusion at the depth of thickness of the material. For adsorption to gypsum and concrete, TCPP may not have diffused to the depth of their thicknesses in the modeled time frame.

Model fit assessment metrics were calculated for the 32 mass transfer related simulations conducted in the sensitivity analysis (Table S.3) and compared to the baseline fit (Simulation 1). The NMSE decreased by at least 1.3 for simulations using both low and high $K_{\text{SPF/a}}$ values and for the simulation using the high C_0 value. All other parameters changed the NMSE by 0.7 or less. Change of $K_{\text{SPF/a}}$ and C_0 also resulted in the largest change in slope (greater than 0.5). The largest changes in correlation coefficient (greater than 0.1) were the result of using both $K_{\text{SPF/a}}$ values, the low $K_{\text{gypsum/a}}$ value and the high D_{SPF} value. The largest intercept changes (>100 %) were the results of using the high $K_{\text{SPF/a}}$, high C_0 , and high D_{SPF} values.

Overall, given the simulation conditions and the parameter variation ranges described above, the predicted TCPP concentration and model fit assessment metrics are more sensitive to mass transfer parameters related to the source (SPF) than the mass transfer parameters related to sinks. Hence, to improve the accuracy of IECCU predictions for TCPP emission

from SPF, more effort is needed to accurately measure and characterize variability of the mass transfer parameters for SPF, especially C_0 and $K_{SPF/a}$. In addition, continued development and refinement of methods to predict model inputs based on available measured data from similar chemicals are recommended (Huang and Jolliet 2019).

Besides improvement of inputs, IECCU itself may also be improved to increase the prediction accuracy. Currently only three conditioned zones are allowed in IECCU. Adding more zones may allow more accurate input of temperatures and interzonal airflows. In addition, when simulating the emission from SPF using the diffusion model in IECCU, only one layer of material is allowed. However, SPF is often covered with gypsum wallboard. Hence, incorporating a diffusion model with multiple layers of materials may broaden the application range of IECCU. In addition, allowing the variation of mass transfer parameters related to sinks with temperature may improve the prediction accuracy. Furthermore, the number of data points that can be output from IECCU are limited to 5 000. Allowing more output datapoints will increase the time resolution of output and allow better comparison between predictions and measurements, especially when the concentration can vary significantly due to diurnal perturbations.

Conclusions

IECCU is the most recently developed USEPA indoor exposure model that can predict chemical emissions from sources and sorption to sinks. To evaluate IECCU, this study compared measured TCPP concentrations from 2013 to 2018 in a test house to IECCU predictions under three simulation conditions combining different building configurations, and different airflow and temperature inputs. Overall, given the best available inputs (Simulation 1), IECCU predicted basement concentrations that were generally higher, but within an order of magnitude, of the measured values (average ratio 2.9, range 0.5 to 8.3), while the predicted concentrations in the living zone were generally lower, but also within an order of magnitude of the measurements. The accuracy of the IECCU predictions from Simulation 1 decreased with time. For Simulation 1, the IECCU predicted concentrations in the basement were 1.4 times higher than the measured values within the first two years, but the ratio increased to 4.7 after five years. This trend of predictive accuracy change may be related to the uncertainty of the inputs. Comparing Simulation 1, with quantified input for temperature and airflow, and Simulation 2, with estimated input for temperature and airflow, demonstrates the importance of accurate temperature and airflow inputs for more accurately predicting concentrations and for better capturing the concentration variations due to perturbations. A sensitivity analysis for 20 input parameters indicated that to improve the accuracy of IECCU predictions for TCPP emission from SPF, efforts are needed to accurately measure the mass transfer parameters for SPF, especially source/air partition coefficient ($K_{SPF/a}$) and the initial concentration of the chemical in the source material (C_0).

Supplementary Material

Refer to Web version on PubMed Central for supplementary material.

References

- (2008). EU RISK ASSESSMENT – TCPP CAS 13674-84-5. European Union. https://echa.europa.eu/documents/10162/13630/trd_rar_ireland_tdcp_en.pdf.
- Ali N, Ibrahim Ismail IM, Kadi MW and Salem Ali Albar HM (2018). “Currently used organophosphate flame retardants determined in the settled dust of masjids and hotels of Saudi Arabia, a new insight into human health implications of dust exposure.” *Environ Sci Process Impacts* 20(5): 798–805. DOI: 10.1039/c8em00014j. [PubMed: 29629467]
- ASHRAE (2010). Standard 62.2–2010: Ventilation and Acceptable Indoor Air Quality in Low-Rise Residential Buildings. Atlanta, American Society of Heating, Refrigerating and Air-Conditioning Engineers, Inc.
- ASHRAE (2017). ASHRAE Handbook Fundamentals. Atlanta, American Society of Heating, Refrigerating and Air-Conditioning Engineers.
- ASTM (2017). D8141–17 Standard Guide for Selecting Volatile Organic Compounds (VOCs) and Semi-Volatile Organic Compounds (SVOCs) Emission Testing Methods to Determine Emission Parameters for Modeling of Indoor Environments, ASTM International. <https://www.astm.org/Standards/D8141.htm>.
- ASTM (2019). D5157–19 Standard Guide for Statistical Evaluation of Indoor Air Quality Models, ASTM International. <https://www.astm.org/Standards/D5157.htm>.
- Bevington C, Guo Z, Hong T, Hubbard H, Wong E, Sleasman K and Hetfield C (2017). A Modeling Approach for Quantifying Exposures from Emissions of Spray Polyurethane Foam Insulation in Indoor Environments. Developing Consensus Standards for Measuring Chemical Emissions from Spray Polyurethane Foam (SPF) Insulation: 199–227.
- Bukowski K, Wysokinski D, Mokra K and Wozniak K (2019). “DNA damage and methylation induced by organophosphate flame retardants: Tris(2-chloroethyl) phosphate and tris(1-chloro-2-propyl) phosphate in human peripheral blood mononuclear cells.” *Human & Experimental Toxicology* 36(6). DOI: 10.1177/0960327119839174.
- Chung KC (1996). “Development and validation of a multizone model for overall indoor air environment prediction.” *HVAC&R Research* 2(4): 376–385.
- Davis MW, Healy WM, Boyd M, Payne WV, Skye H, Ng LC and Ullah T (2014). Monitoring Techniques for the Net-Zero Energy Residential Test Facility. NIST Technical Note 1854, U.S. Department of Commerce 10.6028/NIST.TN.1854.
- Ding J, Deng T, Ye X, Covaci A, Liu J and Yang F (2019). “Urinary metabolites of organophosphate esters and implications for exposure pathways in adolescents from Eastern China.” *Sci Total Environ* 695: 133894. DOI: 10.1016/j.scitotenv.2019.133894. [PubMed: 31425989]
- Dols WS and Polidoro BJ (2015). CONTAM User Guide and Program Documentation, NIST Technical Note 1887, National Institute of Standards and Technology. 10.6028/NIST.TN.1887.
- Emmerich SJ (2001). “Validation of Multizone IAQ Modeling of Residential-Scale Buildings: A Review.” *ASHRAE Transactions* 107(2): 619–628.
- Emmerich SJ, Gorfain JE and Howard-Reed C (2003). “Air and Pollutant Transport from Attached Garages to Residential Living Spaces – Literature Review and Field Tests.” *International Journal of Ventilation* 2(3): 265–276. DOI: 10.1080/14733315.2003.11683670.
- Emmerich SJ, Nabinger SJ, Gupte A and Howard-Reed C (2004). “Validation of multizone IAQ model predictions for tracer gas in a townhouse.” *Building Services Engineering Research and Technology* 25(4): 305–316. DOI: 10.1191/0143624404bt100oa.
- Estill CF, Slone J, Mayer AC, Phillips K, Lu J, Chen IC, Christianson A, Streicher R, Guardia MJ, Jayatilaka N, Ospina M and Calafat AM (2019). “Assessment of spray polyurethane foam worker exposure to organophosphate flame retardants through measures in air, hand wipes, and urine.” *J Occup Environ Hyg* 16(7): 477–488. DOI: 10.1080/15459624.2019.1609004. [PubMed: 31112485]
- European Chemicals Agency. (2020). “Substance Infocard: Tris(2-chloro-1-methylethyl) phosphate.” from <https://echa.europa.eu/substance-information/-/substanceinfo/100.033.766>.
- Fanney AH, Payne V, Ullah T, Ng L, Boyd M, Omar F, Davis M, Skye H, Dougherty B, Polidoro B, Healy W, Kneifel J and Pettit B (2015). “Net-zero and beyond! Design and performance

- of NIST's net-zero energy residential test facility." *Energy and Buildings* 101: 95–109. DOI: 10.1016/j.enbuild.2015.05.002.
- Gong M and Poppendieck D (2019). NIST Technical Note 2040: Measurement of Semi-Volatile Organic Chemical (SVOC) Emission Parameters for Building Materials Using a Solid-Phase Microextraction (SPME)-Based Method, National Institute of Standards and Technology 52. 10.6028/NIST.TN.2040.
- Guo Z (2005). Program PARAMS User's Guide. U.S. Environmental Protection Agency, Office of Research & Development and National Risk Management Research Laboratory. <https://nepis.epa.gov/Exe/ZyPDF.cgi/P1007IYY.PDF?Dockkey=P1007IYY.PDF>.
- Haghighat F and Megri AC (1996). "A Comprehensive Validation of Two Airflow Models - COMIS and CONTAM." *Indoor Air* 6(4): 278–288. DOI: 10.1111/j.1600-0668.1996.00007.x.
- Healy W, Chen TH, Dougherty B, Fanney AH, Ullah T, Payne WV, Ng LC and Omar F. (2018). "Net Zero Energy Residential Test Facility Instrumented Data; Year 1." from <https://pages.nist.gov/netzero/data.html>.
- Healy W, Fanney AH, Dougherty B, Payne WV, Ullah T, Ng LC and Omar F. (2017). "Net Zero Energy Residential Test Facility Instrumented Data; Year 2." from <https://pages.nist.gov/netzero/data.html>.
- Huang L and Jolliet O (2019). "A quantitative structure-property relationship (QSPR) for estimating solid material-air partition coefficients of organic compounds." *Indoor Air* 29(1): 79–88. DOI: 10.1111/ina.12510. [PubMed: 30295963]
- Jayatilaka NK, Restrepo P, Davis Z, Vidal M, Calafat AM and Ospina M (2019). "Quantification of 16 urinary biomarkers of exposure to flame retardants, plasticizers, and organophosphate insecticides for biomonitoring studies." *Chemosphere* 235: 481–491. DOI: 10.1016/j.chemosphere.2019.06.181. [PubMed: 31272008]
- Ji C, Lu Z, Xu L, Li F, Cong M, Shan X and Wu H (2020). "Global responses to tris(1-chloro-2-propyl)phosphate (TCPP) in rockfish *Sebastes schlegeli* using integrated proteomic and metabolomic approach." *Sci Total Environ* 724: 138307. DOI: 10.1016/j.scitotenv.2020.138307. [PubMed: 32272412]
- Kim UJ, Wang Y, Li W and Kannan K (2019). "Occurrence of and human exposure to organophosphate flame retardants/plasticizers in indoor air and dust from various microenvironments in the United States." *Environ Int* 125: 342–349. DOI: 10.1016/j.envint.2019.01.065. [PubMed: 30739054]
- Levi PG and Cullen JM (2018). "Mapping Global Flows of Chemicals: From Fossil Fuel Feedstocks to Chemical Products." *Environ Sci Technol* 52(4): 1725–1734. DOI: 10.1021/acs.est.7b04573. [PubMed: 29363951]
- Liang Y, Liu X and Allen MR (2018). "Measuring and modeling surface sorption dynamics of organophosphate flame retardants on impervious surfaces." *Chemosphere* 193: 754–762. DOI: 10.1016/j.chemosphere.2017.11.080. [PubMed: 29175403]
- Liu X, Allen MR and Roache NF (2016). "Characterization of organophosphorus flame retardants' sorption on building materials and consumer products." *Atmospheric Environment* 140: 333–341. DOI: 10.1016/j.atmosenv.2016.06.019.
- Mokra K, Bukowski K and Wo niak K (2018). "Effects of tris(1-chloro-2-propyl)phosphate and tris(2-chloroethyl)phosphate on cell viability and morphological changes in peripheral blood mononuclear cells (in vitro study)." *Human & Experimental Toxicology* 37(12). DOI: 10.1177/0960327118783529.
- National Center for Biotechnology Information. (2020). "PubChem Tris(1-chloro-2-propyl) phosphate." Retrieved 02/14/2020, 2020, from https://pubchem.ncbi.nlm.nih.gov/compound/Tris_1-chloro-2-propyl_phosphate#section=Color-Form.
- National Toxicology Program (2020). Testing Status of Tris(Chloropropyl) Phosphate (TCPP) M20263. https://ntp.niehs.nih.gov/whatwestudy/testpgm/status/ts-m20263.html?utm_source=direct&utm_medium=prod&utm_campaign=ntpgolinks&utm_term=ts-m20263.
- Ng L, Kinser L, Emmerich SJ and Persily A (2019). Estimating Interzonal Leakage in a Net-Zero Energy House. Symposium on Whole Building Air Leakage: Testing and Building Performance Impacts: 211–229.

- Ng L, Persily A and Emmerich S (2015). Infiltration and Ventilation in a Very Tight, High Performance Home. Proceedings of 36th AIVC, Conference on Effective Ventilation in High Performance Buildings, Madrid, Spain.
- Ospina M, Jayatilaka NK, Wong LY, Restrepo P and Calafat AM (2018). "Exposure to organophosphate flame retardant chemicals in the U.S. general population: Data from the 2013–2014 National Health and Nutrition Examination Survey." *Environ Int* 110: 32–41. DOI: 10.1016/j.envint.2017.10.001. [PubMed: 29102155]
- Peng C, Tan H, Guo Y, Wu Y and Chen D (2017). "Emerging and legacy flame retardants in indoor dust from East China." *Chemosphere* 186: 635–643. DOI: 10.1016/j.chemosphere.2017.08.038. [PubMed: 28818590]
- Percy Z, La Guardia MJ, Xu Y, Hale RC, Dietrich KN, Lanphear BP, Yolton K, Vuong AM, Cecil KM, Braun JM, Xie C and Chen A (2020). "Concentrations and loadings of organophosphate and replacement brominated flame retardants in house dust from the home study during the PBDE phase-out." *Chemosphere* 239: 124701. DOI: 10.1016/j.chemosphere.2019.124701. [PubMed: 31499316]
- Pettit B, Gates C, Fanney AH and Healy W (2014). Design Challenges of the NIST Net-Zero Energy Residential Test Facility. Gaithersburg, MD, National Institute of Standards and Technology: 71. <https://nvlpubs.nist.gov/nistpubs/TechnicalNotes/NIST.TN.1847.pdf>.
- Poppendieck D, Gong M and Emmerich S (2017). NIST Technical Note 1921: Characterization of Emissions from Spray Polyurethane Foam, Final Report to U.S. Consumer Product Safety Commission, NIST. 10.6028/NIST.TN.1921.
- Poppendieck D, Gong M, Ng L, Dougherty B, Pham V and Zimmerman SM (2019). "Applicability of Spray Polyurethane Foam Ventilation Guidelines for Do-It-Yourself Application Events." *Building and Environment* 157: 227–234. DOI: 10.1016/j.buildenv.2019.04.033.
- Poppendieck D, Khurshid S, Dols WS, Ng L, Polidoro B and Emmerich S (2016). Formaldehyde Concentrations in a Net-Zero Energy House: Real-time Monitoring and Simulation. *Indoor Air 2016*, Ghent, Belgium, International Society of Indoor Air Quality and Climate.
- Poppendieck D, Schlegel M, Connor A and Blickley A (2016). Flame Retardant Emissions from Spray Polyurethane Foam Insulation. US Department of Commerce. Content submitted to: ASTM Standard Selected Technical Papers, Indoor Air Quality and Ventilation Group; Engineering Laboratory; Energy and Environment Division; National Institute of Standards and Technology. http://ws680.nist.gov/publication/get_pdf.cfm?pub_id=917144.
- Poppendieck DG, Ng LC, Persily AK and Hodgson AT (2015). "Long term air quality monitoring in a net-zero energy residence designed with low emitting interior products." *Building and Environment* 94: 33–42. DOI: 10.1016/j.buildenv.2015.07.001.
- Schreder ED, Uding N and La Guardia MJ (2016). "Inhalation a significant exposure route for chlorinated organophosphate flame retardants." *Chemosphere* 150: 499–504. DOI: 10.1016/j.chemosphere.2015.11.084. [PubMed: 26775187]
- Sebroski JR (2012). Research Report for Measuring Emissions from Spray Polyurethane Foam (SPF) Insulation. Pittsburgh, PA, Center for the Polyurethanes Industry (CPI): 52. <http://polyurethane.americanchemistry.com/Resources-and-Document-Library/Research-Report-for-Measuring-Emissions-from-Spray-Polyurethane-Foam-SPF-Insulation.pdf>.
- Tan H, Peng C, Guo Y, Wang X, Wu Y and Chen D (2017). "Organophosphate Flame Retardants in House Dust from South China and Related Human Exposure Risks." *Bull Environ Contam Toxicol* 99(3): 344–349. DOI: 10.1007/s00128-017-2120-8. [PubMed: 28573493]
- Tian S, Sebroski J and Ecoff S, Eds. (2017). Predicting TCPP Emissions and Airborne Concentrations from Spray Polyurethane Foam Using USEPA i-SVOC software: Parameter Estimation and Result Interpretation. ASTM STP 1589 — Developing Consensus Standards for Measuring Chemical Emissions from Spray Polyurethane Foam (SPF) Insulation, ASTM.
- Tokumura M, Hatayama R, Tatsu K, Naito T, Takeda T, Raknuzzaman M, Al-Mamun MH and Masunaga S (2017). "Organophosphate flame retardants in the indoor air and dust in cars in Japan." *Environ Monit Assess* 189(2): 48. DOI: 10.1007/s10661-016-5725-1. [PubMed: 28054199]

- United States Environmental Protection Agency. (2020a). "Indoor Semi-volatile Organic Compounds (i-SVOC) Version 1.0." from <https://www.epa.gov/chemical-research/indoor-semi-volatile-organic-compounds-i-svoc-version-10>.
- United States Environmental Protection Agency. (2020b). "Simulation Tool Kit for Indoor Air Quality and Inhalation Exposure (IAQX)." from <https://www.epa.gov/air-research/simulation-tool-kit-indoor-air-quality-and-inhalation-exposure-iaqx>.
- United States Environmental Protection Agency. (2020c). "User's Guide and Download for IECCU-Indoor Environmental Concentrations in Buildings with Conditioned and Unconditioned Zones." Retrieved 05/14/2020, 2020, from <https://www.epa.gov/tsca-screening-tools/users-guide-and-download-ieccu-indoor-environmental-concentrations-buildings>.
- Wang Y, Bao M, Tan F, Qu Z, Zhang Y and Chen J (2020). "Distribution of organophosphate esters between the gas phase and PM2.5 in urban Dalian, China." *Environ Pollut* 259: 113882. DOI: 10.1016/j.envpol.2019.113882. [PubMed: 31926391]
- Wu H, Zhong M, Lu Z, Shan X, Li F, Ji C and Cong M (2018). "Biological effects of tris (1-chloro-2-propyl) phosphate (TCPP) on immunity in mussel *Mytilus galloprovincialis*." *Environ Toxicol Pharmacol* 61: 102–106. DOI: 10.1016/j.etap.2018.05.022. [PubMed: 29879610]
- Wu M, Yu G, Cao Z, Wu D, Liu K, Deng S, Huang J, Wang B and Wang Y (2016). "Characterization and human exposure assessment of organophosphate flame retardants in indoor dust from several microenvironments of Beijing, China." *Chemosphere* 150: 465–471. DOI: 10.1016/j.chemosphere.2015.12.111. [PubMed: 26796586]
- Xu D, Yu K and Qian K (2018). "Thermal degradation study of rigid polyurethane foams containing tris(1-chloro-2-propyl)phosphate and modified aramid fiber." *Polymer Testing* 67: 159–168. DOI: 10.1016/j.polymertesting.2018.01.034.

Highlights

- Airborne tris(1-chloro-2-propyl) phosphate (TCPP) concentrations are detected years after application of spray polyurethane foam (SPF).
- Using measured building parameters improves model performance compared to using default design parameters.
- *Indoor Environmental Concentrations in Buildings with Conditioned and Unconditioned Zones (IECCU)* model predictions can be improved through better parameterizing source-related mass transfer inputs.

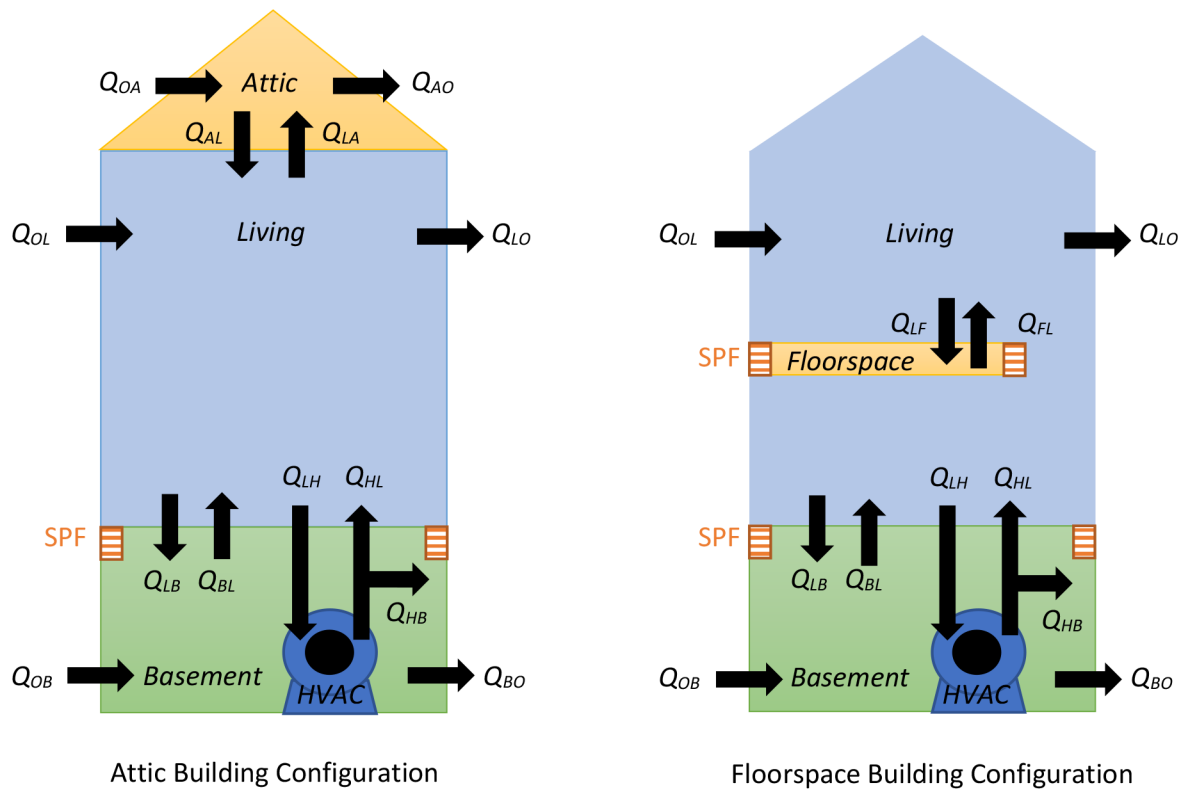


Figure 1. Building configurations used in IECCU simulations. Airflow (Q) subscripts: Outside (O), Attic (A), Living Area (L), Basement (B), HVAC system (H), Floorspace (F).

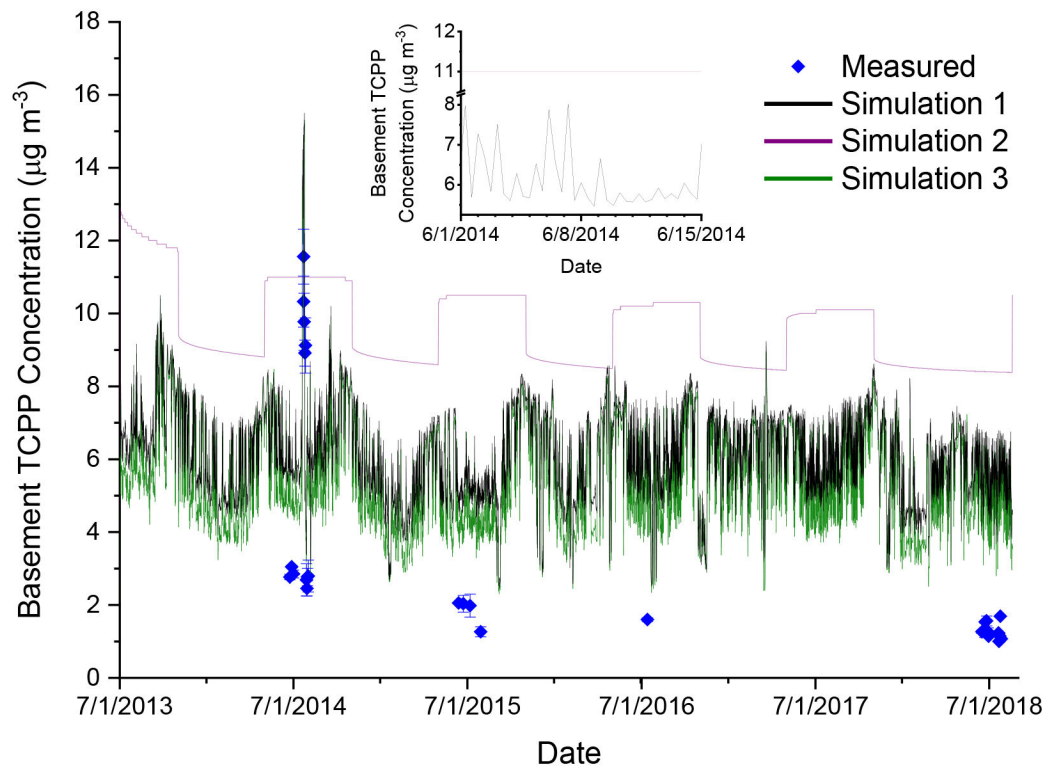


Figure 2. Comparison of TCPP concentrations in the basement simulated using quantified input (Simulation 1, Attic Configuration and Simulation 3, Floorspace Configuration) and estimated input (Simulation 2, Attic Configuration). Error bars on triplicate measured samples represent two standard deviations.

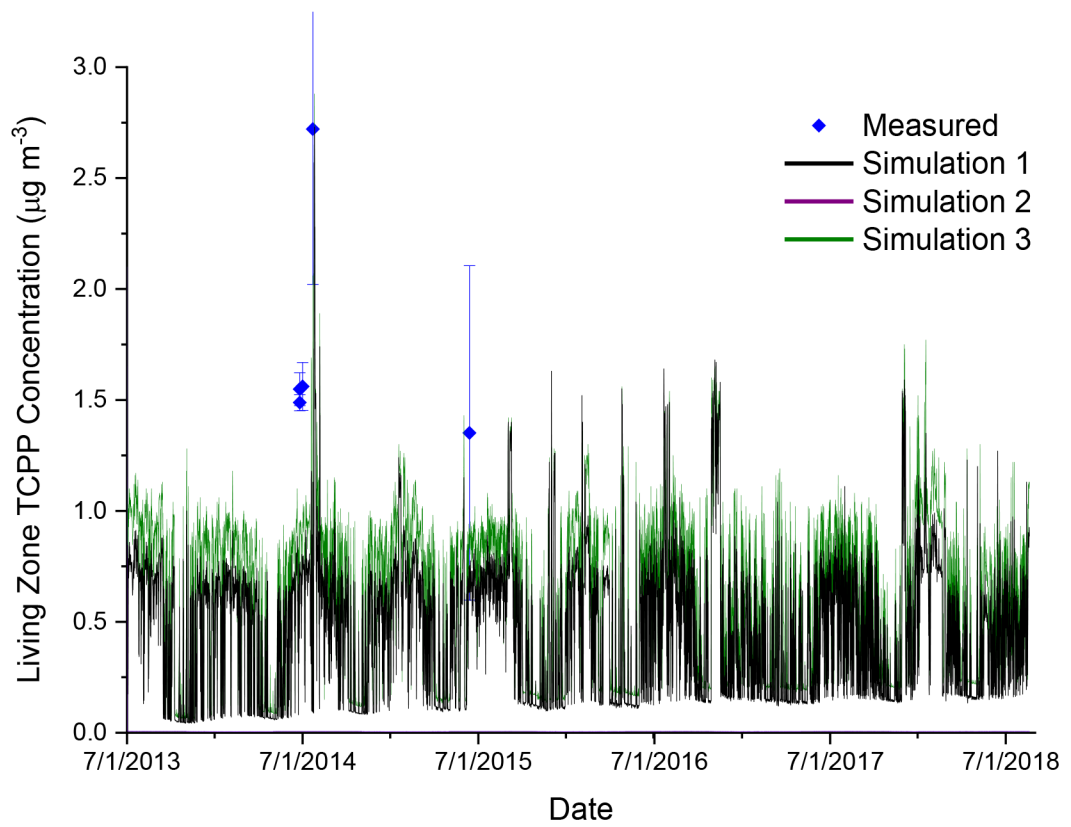


Figure 3. Comparison of living zone TCPP concentrations simulated using measured data, quantified input data (Simulation 1, Attic Configuration and Simulation 3, Floorspace Configuration). Error bars on triplicate measured samples represent two standard deviations.

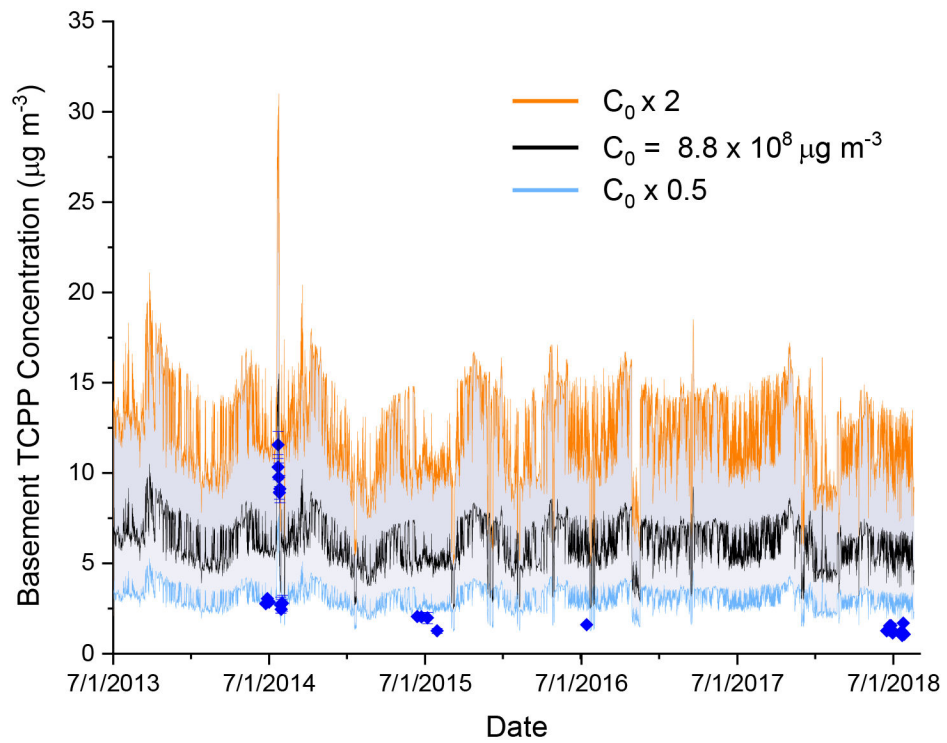


Figure 4. TCPP basement concentration predictions for factor of two changes in the initial TCPP concentration in the SPF. Error bars on triplicate measured samples represent two standard deviations.

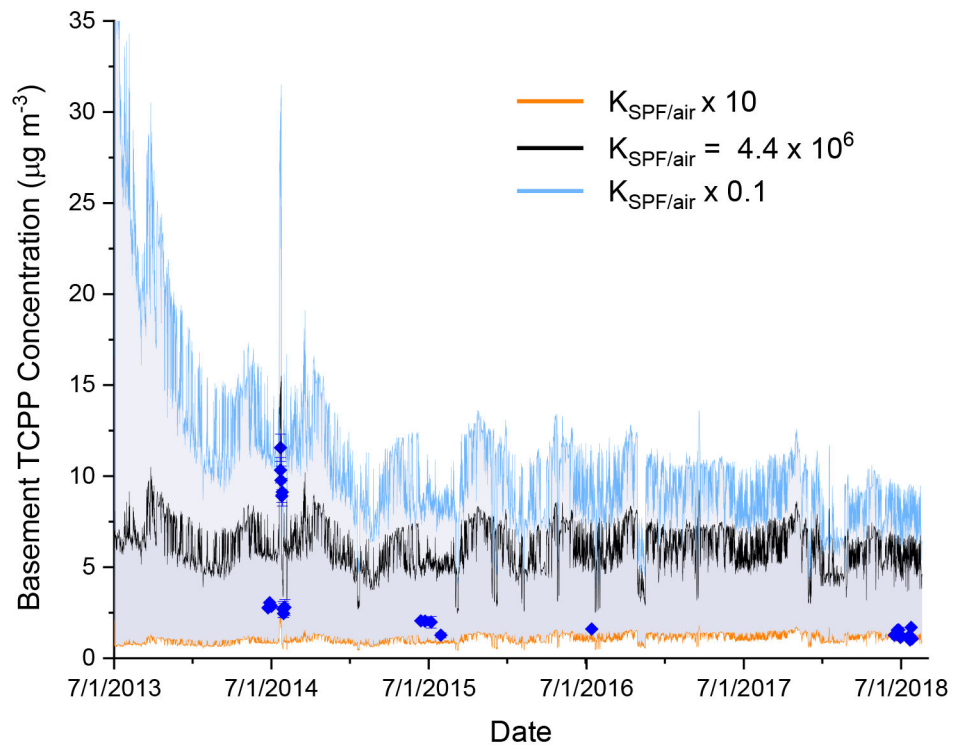


Figure 5. TCPP basement concentration predictions for order of magnitude changes in the SPF partition coefficient. Error bars on triplicate measured samples represent two standard deviations.

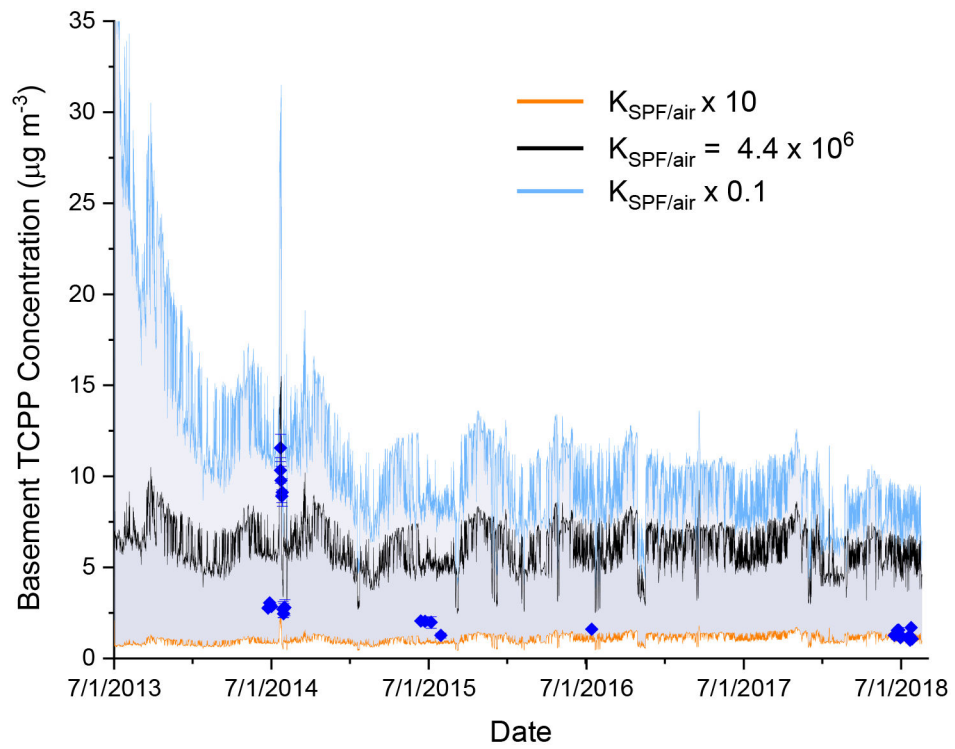


Figure 6. TCPP basement concentration predictions for order of magnitude changes in the SPF diffusion coefficient. Error bars on triplicate measured samples represent two standard deviations.

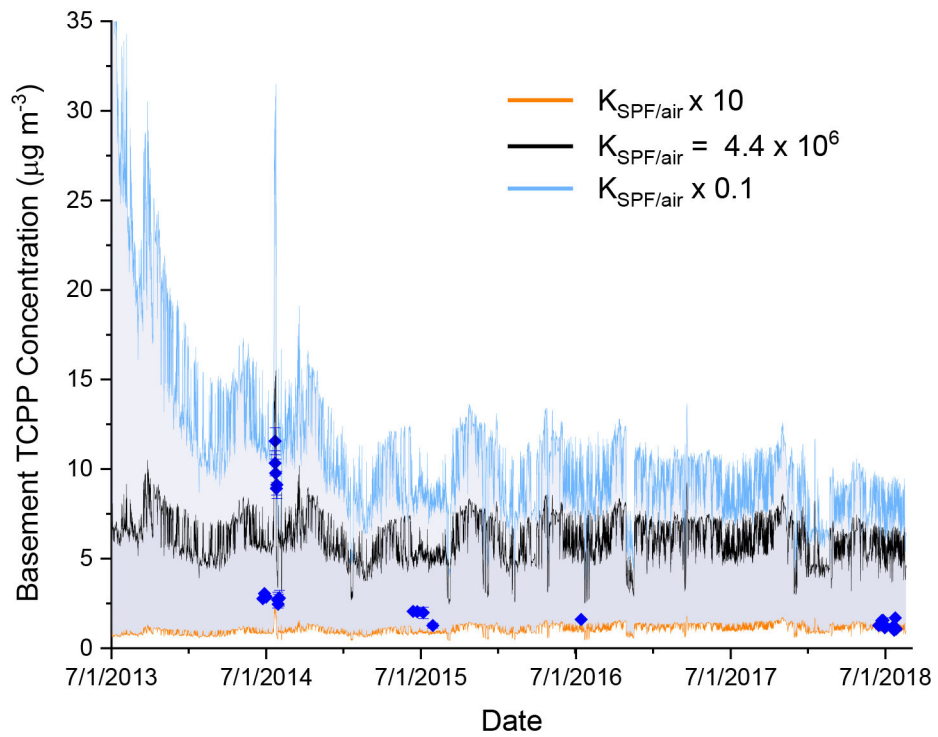


Figure 7. TCPP basement concentration predictions for factor of two changes in the SPF mass transfer coefficient, $h_{m, \text{SPF}}$. Error bars on triplicate measured samples represent two standard deviations.

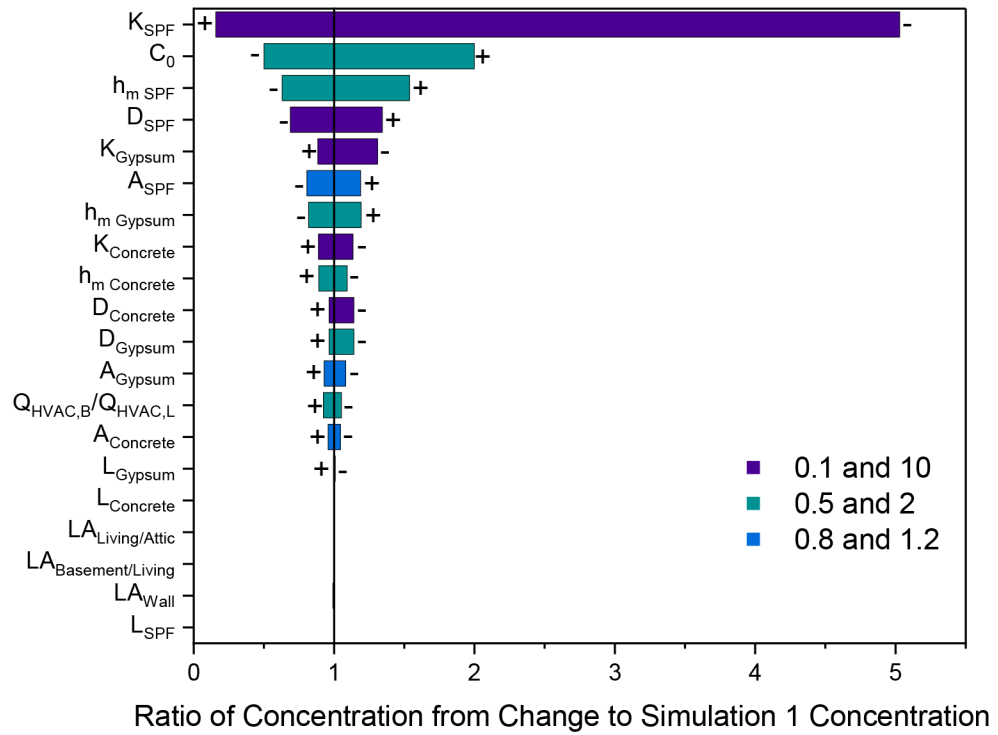


Figure 8. Ratio of average concentration for high and low parameter value and the average concentration from Simulation 1. Positive/negative signs indicate high/low parameter values. Legend refers to the range of values tested. Parameters defined in Table S.2

Table 1.

Simulation building configurations and data sets

Simulation	Building Configuration	Input Data for Building Operations
1	Attic	Quantified
2	Attic	Design
3	Floorspace	Quantified

Table 2.

TCPP and zone size input parameters for IECCU model (at 25 °C)

Parameters	Value	Unit
Volume of building zone		
Attic	159	m ³
Living area (1 st and 2 nd floors)	856	m ³
Floorspace	48	m ³
Basement	460	m ³
HVAC	14.8 ^a	m ³
Source - SPF		
Initial TCPP concentration, C ₀	8.8×10^8	μg m ⁻³
Partition coefficient between SPF and air, K _{SPF/a}	4.4×10^6 ^b	unitless
Diffusion coefficient, D _{SPF}	8.6×10^{-11} ^b	m ² h ⁻¹
Convective mass transfer coefficient, h _{m, spf}	0.81	m h ⁻¹
Exposed surface area – basement, A _{SPF}	15	m ²
Exposed surface area – floorspace	15	m ²
Thickness of SPF, L _{SPF}	0.1	m
Sink - gypsum board		
Partition coefficient between gypsum board and air, K _{gypsum/a}	4.3×10^6 ^b	unitless
Diffusion coefficient, D _{gypsum}	1.7×10^{-9} ^b	m ² h ⁻¹
Convective mass transfer coefficient, h _{m, gypsum}	0.53	m h ⁻¹
Exposed surface area - attic	218	m ²
Exposed surface area - living	959	m ²
Exposed surface area - floorspace	114	m ²
Exposed surface area - basement	165	m ²
Thickness of gypsum, L _{gypsum}	0.012	m
Sink - concrete		
Partition coefficient between concrete and air K _{concrete/a}	5.4×10^6	unitless
Diffusion coefficient, D _{concrete}	3.7×10^{-10}	m ² h ⁻¹
Convective mass transfer coefficient, h _{m, concrete}	0.57	m h ⁻¹
Exposed surface area – basement, A _{concrete}	122	m ²
Thickness of concrete, L _{concrete}	0.1	m

^a 1 % of house volume^b Average of measured values from Liu, Allen et al. (2016)

Table 3.

Model fit parameters for each simulation.

	Simulation 1	Simulation 2	Simulation 3	Range from Sensitivity Analysis of Simulation 1	ASTM Guideline Criteria ^b
Normalized mean square error (NMSE)	0.64	1.31	0.48	0.44 to 4.0	< 0.25
Correlation coefficient	0.66	0.51	0.70	0.47 to 0.76	> 0.9
Slope	0.58	0.17	0.63	0.06 to 1.47	> 0.75, < 1.25
Intercept^a	122%	256%	92%	7% to 271%	< 25%

^a Presented as percentage of average measured concentrations ($\mu\text{g m}^{-3}$)

^b ASTM D5157 (ASTM 2019)